Camera Calibration, Data Segmentation, and Fitting Approaches for a Visual Edge Inspection System

Mark Tratnig[a], Paul O'Leary[b], Helmut Hlobil[c], Johann Reisinger[d]

[a] Christian Doppler Labor für Sensorische Messtechnik, University of Leoben, Peter Tunner Strasse 27, A-8700 Leoben, Austria

[b] Institute for Automation, University of Leoben, Peter Tunner Strasse 27, A-8700 Leoben, Austria

[c, d] Voest-Alpine Mechatronics Ges.m.b.H., A-4031 Linz, Austria

ABSTRACT

The design of edges is very important for many components. In this paper we therefore present a light-sectioning based measurement head, which is suitable for the edge inspection of different workpieces. Beyond the design we also present a new calibration technique for its camera. The calibration is mainly based on several perspective projections, which are successively executed. In each step, the linear system of homogeneous equations is solved by using singular value decomposition. Each mapping is therefore obtained in the least squares sense. Because of the novel design of the calibration device, a high number of reference points can be used for the description of these mappings.

The inspection of a workpiece detail implicates a large amount of data, some of which is useless. To extract the data essential for the fitting routines, a special correlation/regression based template matching is proposed. After the description of the segmentation process we propose a measurement progression, which enables us to obtain a fast and easy perspective correction of the three-dimensional light sectioning data. Finally, a fitting method is presented. Based on singular value decomposition, the data is fitted to the corresponding form of the fillet or chamfer. As the fit is done in the least squares sense, one can obtain statistical information out of the decomposition process.

Keywords: Camera calibration, Edge inspection, Visual inspection, Data segmentation, Fitting

1. INTRODUCTION

Shape and size of edge regions are essential to the functionality and resistivity of many machine-made parts. Piston rings or stressed, pressure casted parts can fail if the edges are not designed and manufactured properly. Although fillets and chamfers appear on almost every machined part, often their size and shape are still inspected manually with patterns and microscopes. In doing so, size and shape are determined subjectively and the measurement process is time consuming. Furthermore, it is often necessary to cut the component apart to inspect the more hidden details. As mentioned above we will present a light-sectioning based measurement head, which is suitable for the edge inspection of different workpieces. The relative compact design of the head allows for very simple mounting on an industrial robot, whereby complex, mass-produced parts can be inspected in a very efficient way. The measuring task can be done quickly, objectively and without contact.

Fillets and chamfers are generally restricted to very small regions of the machined workpiece. To improve the accuracy of the edge inspection, the cameras field of view is relatively small. Due to the fact that a calibrated

Further author information: (Send correspondence to M.T.)
M.T.: mark.tratnig@unileoben.ac.at, Telephone: 011-43-3842-402-5330, http://automation.unileoben.ac.at
P.O.: automation@unileoben.ac.at, Telephone: 011-43-3842-402-5301, http://automation.unileoben.ac.at
H.H.: helmut.hlobil@vatron.com, Telephone: 011-43-70-6585-8413, http://www.vatron.com
J.R.: Johann.Reisinger@vatron.com, Telephone: 011-43-70-6585-8413, http://www.vatron.com

head enables a very flexible and fast processing of the light sectioning profiles, we found a suitable method for the measurement heads camera calibration. Although many different techniques have been published in the last years,[1,2] most cannot be used for our application because of our small field of view (in the range of some millimeters). In addition to having a simple and easy to understand mathematical approach, our calibration technique has the advantage that the measuring head can be used in every orientation, without exception.

Due to the various sizes of fillets and chamfers the inspection of a workpiece detail implicates a large amount of data, some of which is useless. To extract the data essential for the fitting routines, a special correlation/regression based template matching is proposed. This approach will not only search for appropriate data arrangements, it will also recognize the orientation of asymmetrical (e.g. 2x30°) chamfers.

Finally, an example is given to demonstrate the inspection of a chamfer. It will be shown, that the proposed approach allows a robust, low priced, flexible and fast technique to upgrade the quality inspection of machine-made parts.

1.1. Problem statement

Figure 1(a) shows the image of two pressure casted parts. In Figure 1(b) the measurement heads calibration setup is presented.

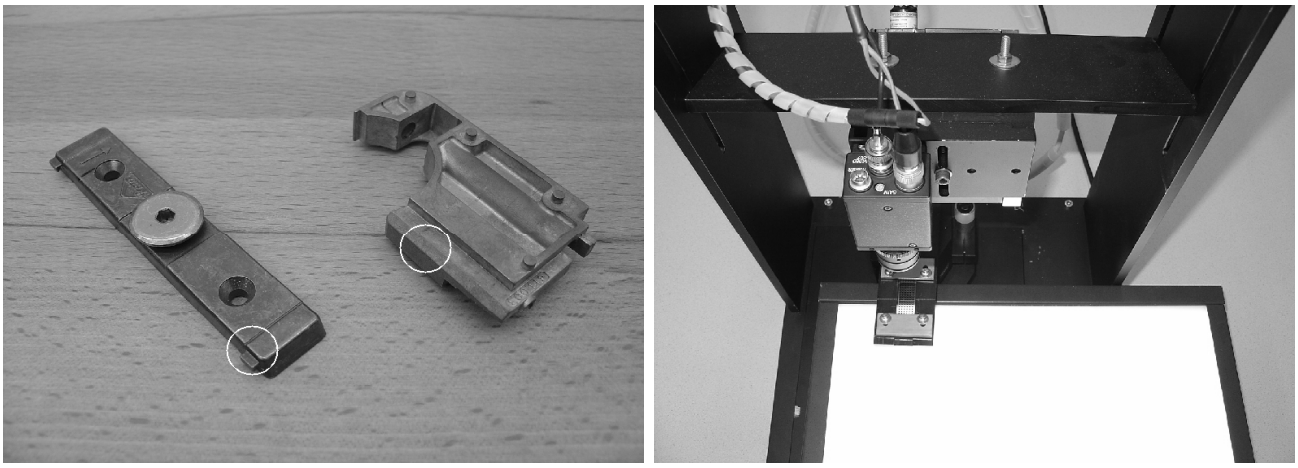

(a) Pressure casted parts, fillet (l.), chamfer (r.)

(b) Measurement heads calibration setup, (top view)

Figure 1. Different workpieces with fillets and chamfers, measurement heads calibration setup

To inspect the marked edge regions in Figure 1(a), the following tasks should be done:

- The measurement heads camera should be calibrated. After this step is carried out, one can get the affine coordinates of the pixel-based light sectioning profile.
- Parts to be inspected should be intersected by the measurement heads laser plane. Calculating the center of gravity (COG) of the captured profile results in a pixel-based representation of the edge region.
- The affine light sectioning profile should be calculated. Afterwards, the profile should be smoothed.
- To extract the essential data, a data segmentation approach should be performed.
- The extracted data should be fitted in the least squares sense.

Using transmitted light techniques, one can also determine the punching geometries. To calibrate the measurements head camera, theses type of illumination has been chosen.

2. CAMERA CALIBRATION

Based on Figure 2(a), the main features of the measurement heads camera calibration should be described first. Simplified, our calibration object consists of at least two parallel planes (calibration planes), whose normal distance h is well known. Beyond this fact, each plane should contain a very precise and correlating grid. It is assumed that there is a coordinate system (fixed coordinate system) attached to the center of an arbitrary point of the lowest grid. Furthermore, another coordinate system (laser coordinate system) is placed in the measurement heads laser plane. By definition, the point of origin is the intersection point of the y-axis of the fixed coordinate system and the laser plane. The x-y-plane of the laser coordinate system is aligned to the laser plane.

The first part of the calibration process determines the position and orientation of the laser plane and its coordinate system relative to the fixed coordinate system. Therefore, the homogeneous projection matrices of the camera plane to all of the calibration planes (stage positions) are required.

The second step in the calibration process determines the homogeneous projection between the laser plane and the camera plane. Given an image points coordinates, one can project this point to its corresponding position in the laser coordinate system. Due to the known orientation of the laser coordinate system, this point can be transformed into the fixed coordinate system. Now existing in affine form, metric measurements can be conducted. Figure 2(b) shows the industrial implementation of the model described above. The device consists

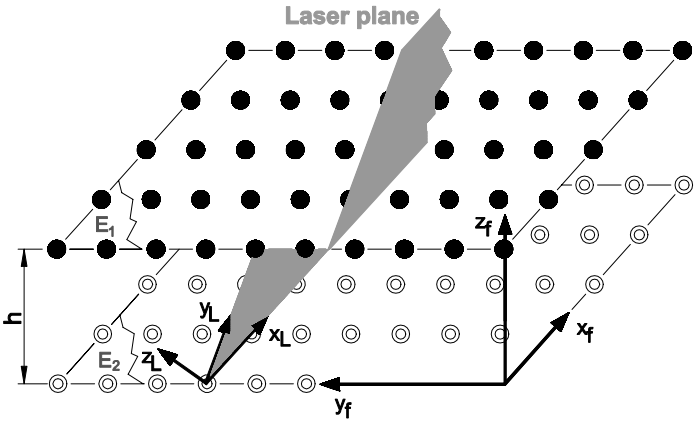

(a) Calibration model

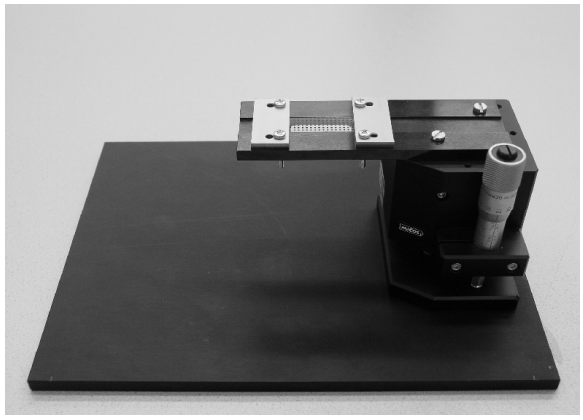

(b) Manually operated elevation stage, grid target

Figure 2. Calibration model, calibration setup

of an accurate grid target, which is vertically moved by a precise elevation stage. The calibration model described in Figure 2(a) can therefore be achieved by a stepwise movement of the target in the vertical direction. Assuming a precise target clamp, the movement of the target can be equate to the normal distance h shown in Figure 2(a).

2.1. Homogeneous Mapping between Camera Plane and Calibration Plane

The homogeneous projection between two points (p_r, p_0) lying in different planes (e.g. E_2 and the camera plane) is usually given by the following equation:

$$\begin{bmatrix} x_r \\ y_r \\ w_r \end{bmatrix} = \begin{bmatrix} h_{11} & h_{12} & h_{13} \\ h_{21} & h_{22} & h_{23} \\ h_{31} & h_{32} & h_{33} \end{bmatrix} \begin{bmatrix} x_0 \\ y_0 \\ 1 \end{bmatrix}, \qquad p_r = \mathrm{H}p_0 \tag{1}$$

Assuming that p_r is the center of a grid point, p_0 is the corresponding center in the captured image. Because one of the nine parameters in H is responsible for the projections scaling, at least four grid points (and their corresponding image points) are required to determine the remaining entities.

Starting with the cameras calibration, the affine coordinates of the grid points should be known. Lying in the fixed coordinate system of Figure 2(a), only the x- and y- components are required. Since Equation 1 is given in homogeneous form, for the affine ([mm]) coordinates of a grid point ($x_{r,a}$, $y_{r,a}$) we have to write:

$$x_{r,a} = \frac{x_r}{w_r} = \frac{h_{11}x_0 + h_{12}y_0 + h_{13}}{h_{31}x_0 + h_{32}y_0 + h_{33}}, \qquad y_{r,a} = \frac{y_r}{w_r} = \frac{h_{21}x_0 + h_{22}y_0 + h_{23}}{h_{31}x_0 + h_{32}y_0 + h_{33}} \tag{2}$$

Rewriting the above formulas to a matrix equation, for n affine points (to decrease the influence of noisy data, more than 4 points should be chosen) we can write:

$$\begin{bmatrix} -x_0^{(1)} & -y_0^{(1)} & -1 & 0 & 0 & 0 & x_{r,a}^{(1)}x_0^{(1)} & x_{r,a}^{(1)}y_0^{(1)} & x_{r,a}^{(1)} \\ 0 & 0 & 0 & -x_0^{(1)} & -y_0^{(1)} & -1 & y_{r,a}^{(1)}x_0^{(1)} & y_{r,a}^{(1)}y_0^{(1)} & y_{r,a}^{(1)} \\ \vdots & \vdots & \vdots & \vdots & \vdots & \vdots & \vdots & \vdots & \vdots \\ -x_0^{(n)} & -y_0^{(n)} & -1 & 0 & 0 & 0 & x_{r,a}^{(n)}x_0^{(n)} & x_{r,a}^{(n)}y_0^{(n)} & x_{r,a}^{(n)} \\ 0 & 0 & 0 & -x_0^{(n)} & -y_0^{(n)} & -1 & y_{r,a}^{(n)}x_0^{(n)} & y_{r,a}^{(n)}y_0^{(n)} & y_{r,a}^{(n)} \end{bmatrix} \begin{bmatrix} h_{11} \\ h_{12} \\ h_{13} \\ h_{21} \\ h_{22} \\ h_{23} \\ h_{31} \\ h_{32} \\ h_{33} \end{bmatrix} = 0, \qquad \mathrm{T}h = 0 \tag{3}$$

To find a non-trivial solution for h_{11} - h_{33}, singular value decomposition[3, 4] can be applied[5] on matrix T. The obtained coefficients h minimize the mean square residual in Equation 3. If noisy data is used, the homogeneous projection H is therefore calculated in the least squares sense. Using *Matlab*, one can derive the coefficients using the following code:

$$\left[\text{ u,s,v } \right] = \mathrm{svd(T)}; \qquad h = \mathrm{v}(:, end); \tag{4}$$

After the coefficients of H have been determined, any image point (p_0) can be projected into the according plane. Using Equation 2, this step can be done very easily. Having m stage positions, we finally get m homogeneous projections H_n, n=1...m.

2.2. Determination of the Laser Plane, Laser Coordinate System

The targets clamp (shown in Figure 2(b)) was manufactured in such a way, that the glass discs upper surface and the clamps top side are coplanar. Based on this arrangement, the measurement heads laser intersects the different target planes in a visible way.

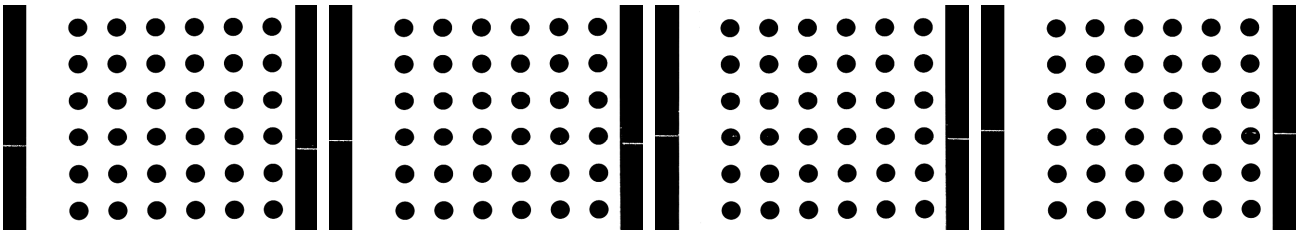

(a) Stage position: 10.75mm (b) Stage position: 11.00mm (c) Stage position: 11.25mm (d) Stage position: 11.50mm

Figure 3. Calibration images at different stage positions

In Figure 3, a set of calibration images is presented. The black dots correspond to the calibration grids of Figure 2(a). Considering the laser line region of an image, one can obtain the intersection profile in the images coordinate system by using a COG-approach.[6] As mentioned above, there is a different homogeneous projection H_n for each stage position (for each calibration picture). Using Equation 2, the two-dimensional affine intersection

profile for each image can be found. Knowing the z-position of the corresponding stage position, the intersection profile is fully determined.

Repeating this procedure for each calibration image will lead us to the spatial description of the laser plane in the fixed coordinate system. Considering a set of n points x_i:y_i:z_i:1 for which the least mean square fit to a plane has to be determined:

$$E_1 x_i + E_2 y_i + E_3 z_i + E_4 = e_i \neq 0; \tag{5}$$

This can be formulated as:

$$\begin{bmatrix} x_1 & y_1 & z_1 & 1 \\ x_2 & y_2 & z_2 & 1 \\ x_3 & y_3 & z_3 & 1 \\ x_4 & y_4 & z_4 & 1 \\ \vdots & \vdots & \vdots & \vdots \\ x_n & y_n & z_n & 1 \end{bmatrix} \begin{bmatrix} N_1 \\ N_2 \\ N_3 \\ N_4 \end{bmatrix} = \begin{bmatrix} e_1 \\ e_2 \\ \vdots \\ e_n \end{bmatrix}, \quad \mathrm{M}N = e \tag{6}$$

Since Equation 6 is an over constrained system, the least mean square solution can be found by setting the error vector e_i=0 and applying singular value decomposition to the matrix M. By the way, it is good practice to use mean free data to reduce the effects of numerical errors. Using *Matlab*, the coefficients can be obtained in the following way:

$$\left[\text{ u,s,v } \right] = \mathrm{svd(M)}; \qquad N = \mathrm{v}(:, end); \tag{7}$$

The resulting equation of the laser plane (in the fixed coordinate system) can now be written in the following way:

$$N_1 x_i + N_2 y_i + N_3 z_i + N_4 = 0 \tag{8}$$

To obtain the position and orientation of the laser coordinate system in the fixed coordinate system, N_1 to N_4 can be used. Because the laser coordinate systems origin is the intersection point of the fixed coordinate systems y-axis and the laser plane (see Figure2(a)), the translation matrix (in homogeneous form) can be written as follows:

$$T = \begin{bmatrix} 1 & 0 & 0 & 0 \\ 0 & 1 & 0 & -(-\frac{N_4}{N_2}) \\ 0 & 0 & 1 & 0 \\ 0 & 0 & 0 & 1 \end{bmatrix} \tag{9}$$

The orientation of the laser coordinate system can be described by the following matrices:

$$R_x = \begin{bmatrix} 1 & 0 & 0 & 0 \\ 0 & cos(-\varphi_x) & -sin(-\varphi_x) & 0 \\ 0 & sin(-\varphi_x) & cos(-\varphi_x) & 0 \\ 0 & 0 & 0 & 1 \end{bmatrix} \quad R_y = \begin{bmatrix} cos(-\varphi_y) & 0 & sin(-\varphi_y) & 0 \\ 0 & 1 & 0 & 0 \\ -sin(-\varphi_y) & 0 & cos(-\varphi_y) & 0 \\ 0 & 0 & 0 & 1 \end{bmatrix} \quad R_z = \begin{bmatrix} cos(-\varphi_z) & -sin(-\varphi_z) & 0 & 0 \\ sin(-\varphi_z) & cos(-\varphi_z) & 0 & 0 \\ 0 & 0 & 1 & 0 \\ 0 & 0 & 0 & 1 \end{bmatrix} \tag{10}$$

To get φ_x, the equation of the intersection line between the laser plane and the y-z-plane of the fixed coordinate system is calculated. Setting x = 0 results in:

$$N_2 y + N_3 z + N_4 = 0 \tag{11}$$

Since φ_x is the slope of this intersection line, one can write:

$$\varphi_x = \arctan(-\frac{N_2}{N_3}) \tag{12}$$

Now the laser coordinate system should be rotated around its y-axis. The angle φ_y corresponds exactly with the angle between $[0,N_2,N_3]^T$ (the direction of the current z-axis) and the normal vector of the laser plane $[N_1,N_2,N_3]^T$. The rotation around the z-axis (φ_z) is inessential and can be set to zero.

To transform a homogeneous point P_{FCS} (P_{FCS}=x_{FCS}:y_{FCS}:z_{FCS}:1) from the fixed coordinate system into the laser coordinate system, the following equation should be used:

$$P_{LCS} = R_z R_y R_x T \begin{bmatrix} x_{FCS} \\ y_{FCS} \\ z_{FCS} \\ 1 \end{bmatrix} \tag{13}$$

To re-transform a point (from the laser coordinate system into the fixed coordinate system), two modifications should be carried out. First, the signs of φ_x, φ_y and $(-\frac{N_4}{N_2})$ should be switched. Having inserted them into R_x, R_y and T, the formula for the re-transformation of a point can be written as follows:

$$P_{FCS} = T R_x R_y R_z \begin{bmatrix} x_{LCS} \\ y_{LCS} \\ z_{LCS} \\ 1 \end{bmatrix} \tag{14}$$

2.3. Homogeneous Mapping between Laser Plane and Camera Plane

To determine the homogeneous mapping between the laser plane and the camera plane, at least 4 points are required. However, we will use a higher number of points. Each calibration image (see Figure 3) contains two laser line segments. Choosing two points per line segment, we will get a total number of 4×(number of calibration images) points to determine the mapping. For the calibration setup presented in Figure 3 those points are shown in the following graph as crosses:

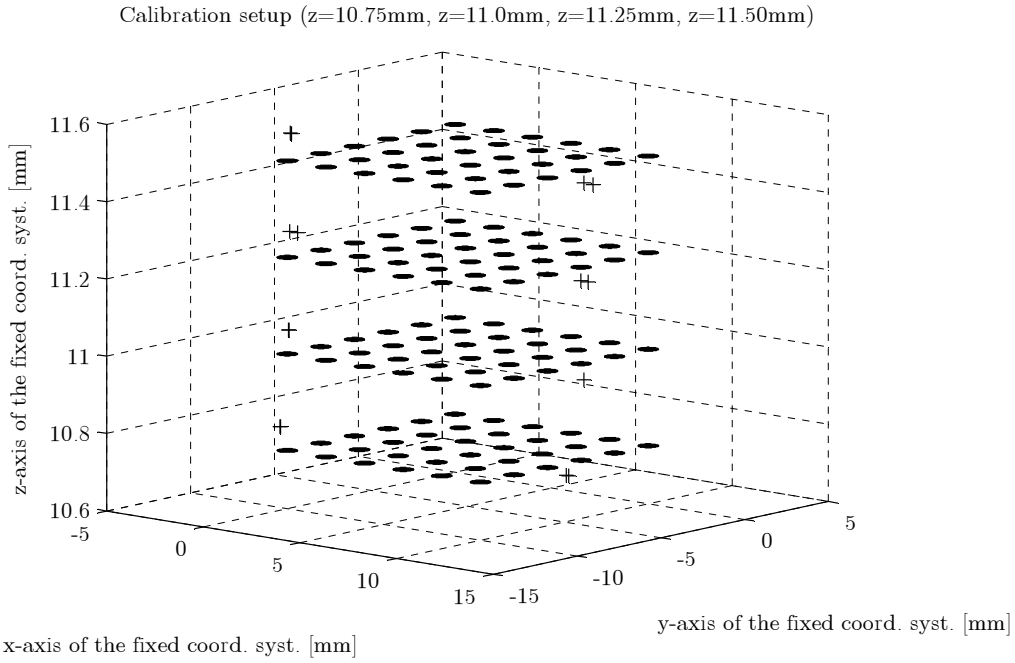

Figure 4. Calibration grids at different stage positions

It has to be noticed that the mentioned points are part of the data which was used to fit the laser plane. More precisely, they are those points of the lines segments, which have the least error concerning the fit. Having an over constrained system, the mapping can be calculated as described in Equation 3.

As mentioned above, one can now project an image point to its corresponding position in the laser coordinate system. Using Equation 14, this point can be transformed into the fixed coordinate system.

3. DATA SEGMENTATION AND FITTING APPROACHES

After describing the measurement heads camera calibration (from now on every movement of the laser relative to the camera is prohibited), we will now present the data segmentation and fitting approaches.

Removing the calibration stage, the measurement head can now inspect the pressure casted parts shown in Figure 1(a). In Figure 5(a) one can see the light sectioning profile of the chamfer, whereas Figure 5(b) presents the sectioning profiles x-z-coordinates in the fixed coordinate system. To obtain this figure, a calibrated measurement head is required.

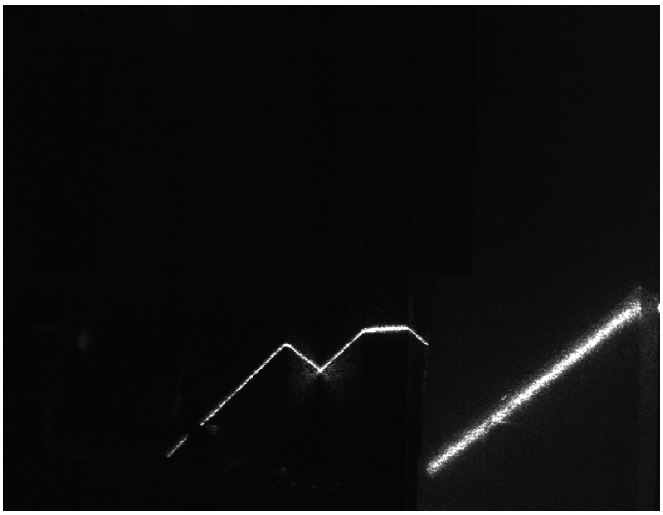

(a) Light sectioning profile of a chamfer

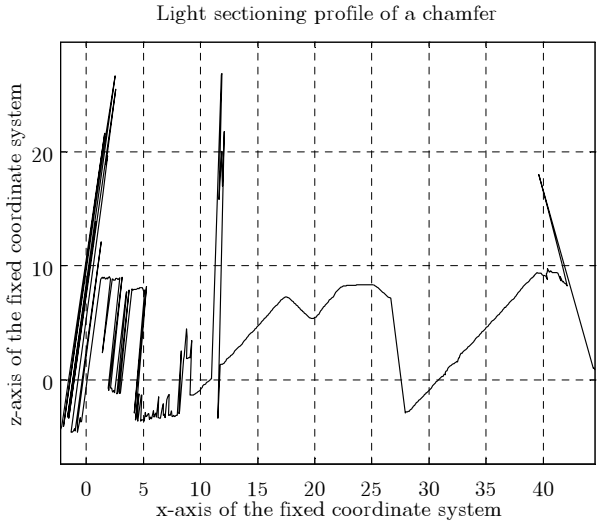

(b) Light sectioning profile in the fixed coord. system

Figure 5. Light sectioning profile of a chamfer (workpiece shown in Figure 1(a))

Concerning Figure 5(b), two things should be noticed. First, one can wonder about the skewed peaks in the profile. Coming from image points with low intensity (lying far away from the correct sectioning profile), they will be discarded in the next step. Furthermore, the wide dimensions of the plotted data will attract attention. Although our calibration technique allows a very small field of view (in the range of some millimeters, e.g. 4-15[mm] field width), the functionality of the data segmentation will be shown on a more comprehensive amount of data.

After the sectioning profile was obtained, the data is smoothed in z-direction. In doing so, image points with low intensity will be discarded. Further, for n = 3 ... n_{max} (n_{max} = number of points - 3), the following Moving Average Filter can be deployed:

$$x_{n,new} = x_n, \qquad z_{n,new} = \frac{1}{5}\sum_{i=-2}^{i=+2} z_{n+i}, \tag{15}$$

For the following segmentation we will need a certain a priori information. Since workpieces can have a very complicated shape, a light sectioning profile can contain several different chamfers. To extract the right one, the chamfers width and angle should be approximately known. It should also be known if the chamfer is forming a inner or an outer edge.

Based on this information, a special template can be generated. As shown in Figure 6(a), the template corresponds to certain parts of the pictured chamfer. Moreover, the figure also shows the results of the smoothing process. In addition to a significant data reduction (the intersection profile has lost about 30 percent of its data points), one can also detect a relevant reduction of the number of peaks.

Starting with the template matching, first the required formulas should be presented. To compare template and light sectioning profile, we will use cross correlation[7] and regression. The correlation between two distributions (e.g. the template and its corresponding part of the sectioning profile) can be computed according to:

$$r_{z_1 z_2} = \frac{\frac{1}{n-1}\sum_{i=1}^{i=n}(z_{1_i} - \overline{z}_1)^2(z_{2_i} - \overline{z}_2)^2}{\sqrt{\frac{1}{n-1}\sum_{i=1}^{i=n}(z_{1_i} - \overline{z}_1)^2}\sqrt{\frac{1}{n-1}\sum_{i=1}^{i=n}(z_{2_i} - \overline{z}_2)^2}}, \qquad -1 \leq r_{z_1 z_2} \leq 1 \tag{16}$$

where $r_{z_1 z_2}$ is called correlation coefficient and n correspond to the the size of the template (number of data points). Furthermore, the z-coordinates of the template are stored in z_1, whereas the z-coordinates of the light sectioning profile can be found in z_2. To obtain the correlation information for the complete profile, the template must be shifted along the whole length.

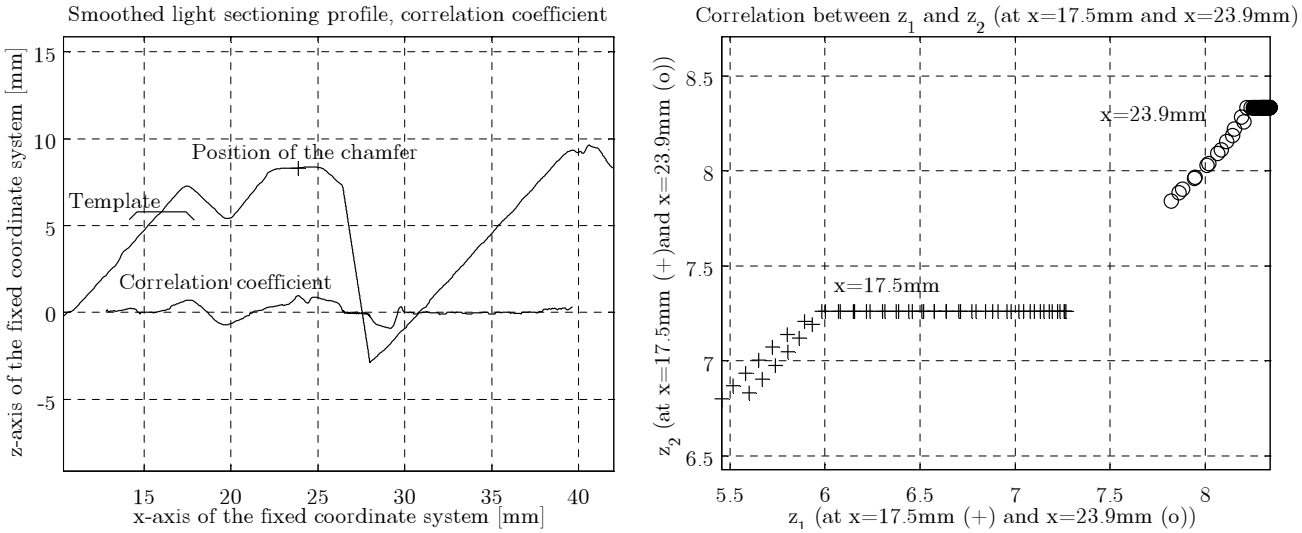

(a) Light sectioning profile, correlation coefficient

(b) Correlating data of template and sectioning profile

Figure 6. Correlation coefficient, correlating data of template and sectioning profile

As can be seen in Figure 6(a), the knowledge of the correlation coefficient is not sufficient to obtain a chamfers position. Considering the light sectioning profile, there can exist several places where the linear interrelation is relatively strong.

Examples are x = 17.5mm and x = 23.9mm in Figure 6(a). For this positions the data distributions are shown in Figure 6(b). As mentioned above, z_1 are the z-coordinates of the templates data points, whereas z_2 are the z-coordinates of the light sectioning profile (of the corresponding part, obviously). As the data points in both cases are aligned quite precisely, one can obtain a relatively strong correlation for both locations.

By calculating the regression coefficient of the correlating data points (z_1, z_2) we directly obtain the slope of the scattered data. One can calculate the regression coefficient in the following way:

$$a = \frac{\frac{1}{n-1}\sum_{i=1}^{i=n}(z_{1_i} - \overline{z}_1)^2(z_{2_i} - \overline{z}_2)^2}{\frac{1}{n-1}\sum_{i=1}^{i=n}(z_{1_i} - \overline{z}_1)^2}, \tag{17}$$

As shown in Figure 6(b), the regression coefficient (the slope) is near to 1 where the template and the light sectioning profile match very good (at x = 23.9mm in Figure 6(a)). Figure 7(a) shows the regression coefficient along the whole light sectioning profile.

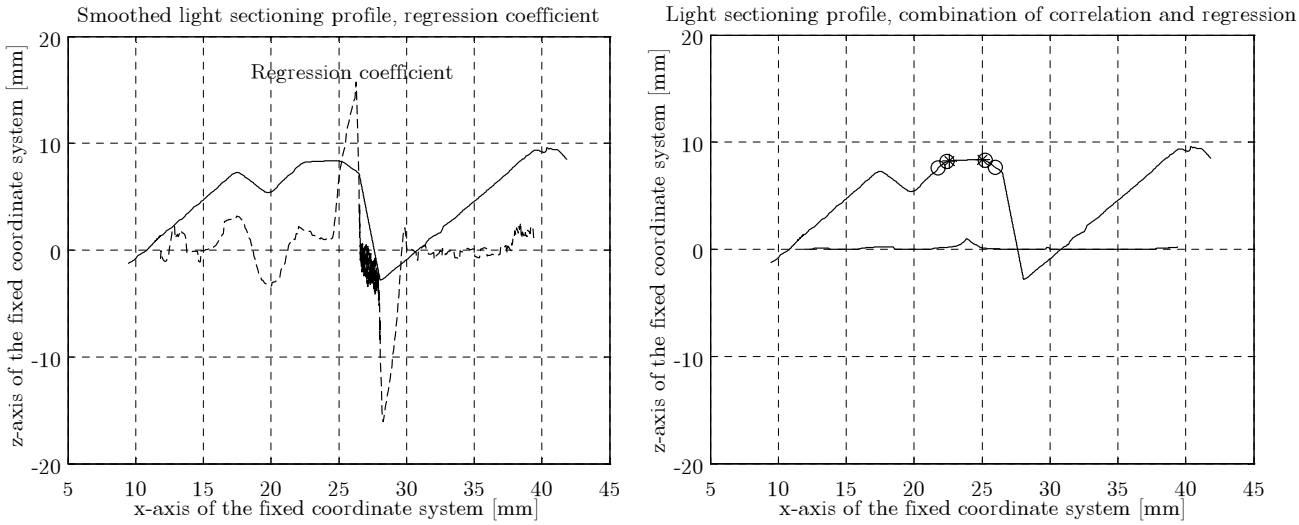

(a) Light sectioning profile, regression coefficient

(b) Combination of correlation and regression

Figure 7. Regression coefficient, combination of correlation and regression

To get a reliable estimation of the chamfers position, we will now combine both types of coefficients in the following way:

$$C_{comb} = t \cdot b \tag{18}$$

where

$$t = \begin{cases} r_{xy} & for \quad 0 < r_{xy} < +1 \\ 0 & for \quad -1 < r_{xy} \leq 0 \end{cases} \tag{19}$$

and

$$b = \begin{cases} a & for \quad a \leq +1 \\ \frac{1}{a} & for \quad a > +1 \end{cases} \tag{20}$$

The result can be seen in Figure 7(b). The combined coefficient C_{comb} reaches values between 0 and 1, whereupon the position of the maxima indicates the chamfers location. In Figure 7(b), the chamfer was found very clear.

After the position of the chamfer has been calculated, one can use the a-priori information to roughly estimate the borders of the chamfers top side. To get a more accurate result, an iterative line fitting approach can be used. Deciding an error margin for the distance between a data point and the fitted line, the borders of all three chamfer planes can be found.

In Figure7(b), the estimated borders of the chamfer has been plotted. In the spatial sense there are three planes, covering approximately the following sections: x = 21.8mm-22.4mm (the left plane), x = 22.6mm-25.0mm (the center plane) and x = 25.2mm-26.0mm (the right plane). To recognize breaks in the sectioning profile, the above mentioned error margin had to be set to a very low value. Although the left plane is very narrow, this reduction will not cause a problem.

To correct the perspective, at least two sectioning profiles are required. Having three of them (they have to be displaced in the fixed coordinates y-direction), we will get a satisfying amount of data to fit the chamfer. Determining the line of intersection between the chamfers left and right plane will lead to the spatial direction of the edge. Assuming a plane perpendicular to the intersection line, a transformation in this plane will cause a rectification. Figure 8(a) shows the corrected light sectioning profiles.

After this steps are carried out (the offset of the sectioning profiles must also be considered), one can fit the data like shown in Equation 6. Getting three planes in parametric form, their orthogonal vectors can be used to determine the chamfers angle. Furthermore, the fitted planes can be used to calculate the chamfers width. In Figure 8(b), the fitted chamfer is presented.

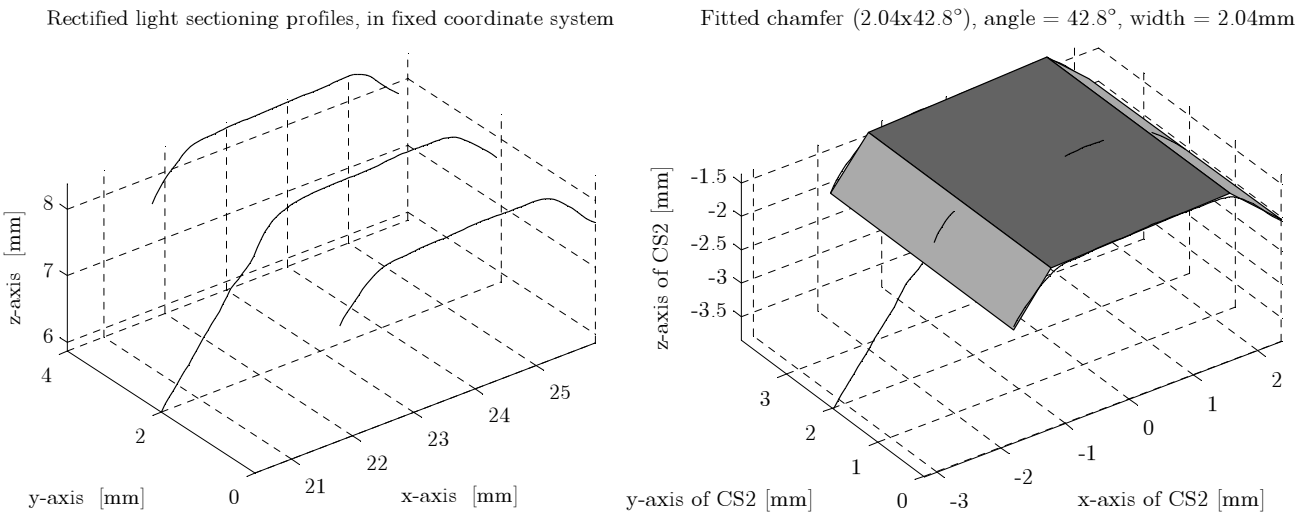

(a) Rectified light sectioning profiles

(b) Fitted chamfer (2.04x42.8°)

Figure 8. Rectified light sectioning profiles, fitted chamfer, results

4. CONCLUSIONS AND RESULTS

An enhanced algorithm for the calibration of a light-sectioning based measurement head has been shown. Beyond the calibration method, we have also presented a suitable calibration target. The application of singular value decomposition has been proposed as a method to fit data. Furthermore, a statistical approach for data segmentation was presented, which was used to extract the measurement data out of the total light-sectioning data. Finally, rectification and fitting approaches have been described. An example has been given to demonstrate the full functionality of the method. Although we only presented the inspection of a chamfer, one can easily expand the principle to other shapes.

Verifications regarding the accuracy have been carried out in former times.[8] Using a conventional CCD camera (a resolution of 24μm per pixel was obtained) a 2-mm calliper was inspected 15 times. Achieving an average width of 2.004 mm (with a variance of $1.74{\cdot}10^{-5}mm^2$), the verification of accuracy has satisfied.

REFERENCES

1. A. Sommerfelt and T. Melen, *A Simple Method for Calibrating Sheet-of-Light Triangulation Systems*, SINTEF Instrumentation, N-0314 Oslo, Norway, 1996.
2. T. Melen and A. Sommerfelt, *Calibrating Sheet-of-Light Triangulation Systems*, SINTEF Instrumentation, N-0314 Oslo, Norway, 1996.
3. G. Golup and C. V. Loan, *Matrix Computations*, The John Hopkins University Press, 1996.
4. C. L. Lawson and R. J. Hanson, *Solving Least Squares Problems*, Prentice Hall, 1974.
5. P. O'Leary, *Fitting Geomteric Models in Image Processing using Grassmann Manifolds*, Proceedings of the SPIE conference, Machine Vision Applications in Industrial Inspections X, San Jose (USA), 2002.
6. A. Gustafsson, *A Study of Subpixel Accuracy using Center of Gravity Estimations*, Report No. LiTH-ISY-R-2000, Linköpings University, Sweden, 1998.
7. Y.-W. Chang, "A signal pattern matching and verification method using interval means cross correlation and eigenvalues in the nuclear power plant monitoring systems," **29**, pp. 1795–1807, Annals of Nuclear Energy, 2002.
8. M. Tratnig, *Makroobjektiv-Lichtschnittmesskopf, Prüfungen und Statistische Auswertungen*, Christian Doppler Labor für Sensorische Messtechnik, University of Leoben, A-8700 Leoben, Austria, 2003.